

Mediterranean Sea, neglecting solar and/or advection evolution, is $Q_{\text{tot}} = -dQ_c - dQ_e - dQ_n$ or, expressed as a function of dT_s and dT_a (with $Q_{T_{\text{sw}}} = 15 dT_s$), $x dC = 0.7 + 63.7 dT_s - 41.8 dT_a$.

From the previous estimates of dT_s ($20 \times 10^{-3} \text{ }^\circ\text{C yr}^{-1}$), the greenhouse effect is zero if the air warming (driven by processes outside of the basin) is $\sim 5 \times 10^{-2} \text{ }^\circ\text{C yr}^{-1}$, eight times the mean global change¹⁰. Inversely, the maximum calculated greenhouse effect (for $dT_a = 0$) is 2 W m^{-2} . But, in the Mediterranean Sea, an area almost without external thermal advection, sea surface and air temperatures are likely to change similarly, as previously shown at a global scale¹². An upper estimate of dT_a is dT_s and a lower estimate is the global evolution of T_a (ref. 10). These temperatures determine a greenhouse effect over the Mediterranean Sea of $1.1\text{--}1.7 \text{ W m}^{-2}$.

These effects represent an evolution of 2% in Q_n , which acts to warm the sea and to a lesser extent to increase the sensible and latent transfers. Consequently, for a dT_a of $6 \times 10^{-3} \text{ }^\circ\text{C yr}^{-1}$, salinity increases by 2×10^{-3} p.s.u. yr^{-1} in the surface layer. A temperature-type calculation links the salinity change in the deep layer to a surface salinity increase of $\sim 5 \times 10^{-3}$ p.s.u. yr^{-1} , which requires, besides the evaporation effect, a reduction of mean freshwater input by $\sim 2\%$ for a further salinity effect of 3×10^{-3} p.s.u. yr^{-1} . On the scale of the whole sea, the high spatial and temporal variability of precipitation prevents any direct evidence of a general decrease, but analysis of data acquired at Monaco between years 1911 and 1985¹³ shows decreasing precipitation which, during the past 30 years, reduced the mean freshwater input by 7%. The marine estimated greenhouse effect is slightly lower than the global value 1.9 W m^{-2} calculated from the evolution of the radiative-gas concentration in the atmosphere since 1860¹⁴. The dynamical coupling of the two large eastern and western basins, where the deep waters have different residence times (about 20 years in the western basin and 50 years in the eastern basin), may somewhat reduce the deep thermal evolution when the driving force is not steady. For instance, the global change dT_a (ref. 10) shows a stagnation between 1940 and 1965, which, if it applies to the Mediterranean area, may result in a constant temperature in the intermediate layer during the past decade. Moreover, some new flow values are smaller than ours (annual Atlantic surface inflow of $41 \times 10^{12} \text{ m}^3 \text{ yr}^{-1}$ (ref. 15), and deep outflow of $27 \times 10^{12} \text{ m}^3 \text{ yr}^{-1}$ for a mean outflow salinity of 37.9 p.s.u. (ref. 16), instead of our values 53 and $50 \times 10^{12} \text{ m}^3 \text{ yr}^{-1}$, respectively); these would lead to an increase in the surface warming and the calculated greenhouse effect would reach maximum values (for $dT_a = 0$) of 2.3 and 2.6 W m^{-2} respectively, not very different from our value of 2 W m^{-2} . Nevertheless, the Mediterranean Sea offers the opportunity to quantify the climate changes and particularly the greenhouse effect through the temperature change in the western deep water. This homogeneous deep water constitutes a rather stable integrating medium and oceanographic measurements may complement the atmospheric experiments, which are complicated by high spatio-temporal variabilities of climate. \square

Received 17 April; accepted 22 August 1990.

- Lacombe, H., Tchernia, P. & Gamberoni, L. *Prog. Oceanogr.* **14**, 319–338 (1985).
- Bethoux, J. P. thesis Univ. Paris (1977).
- Bethoux, J. P. *Oceanol. Acta* **3**, 79–88 (1980).
- Medoc Group *Nature* **227**, 1037–1040 (1970).
- Tchernia, P. *Colloques Int. CNRS* **215**, 17–21 (1974).
- Cane, M. A. *Science* **222**, 1189–1195 (1983).
- Brewer, P. G. et al. *Science* **222**, 1237–1239 (1983).
- Roemmich, D. & Wunsch, C. *Nature* **307**, 447–450 (1984).
- Lazier, J. R. N. *Deep Sea Res.* **35**, 1247–1253 (1988).
- Jones, P. D. et al. *Nature* **332**, 790 (1988).
- Laevastu, T. *Soc. Sci. Fennica* **25**, 1–136 (1960).
- Folland, C. K., Parker, D. E. & Kates, F. E. *Nature* **310**, 670–673 (1984).
- Un siècle d'observations météorologiques à Monaco* Vol. 3 (Centre Scientifique de Monaco, Monaco, 1988).
- Mitchell, J. F. B. *Rev. Geophys.* **27**, 115–139 (1989).
- Perkins, H., Kinder, T. & La Violette, P. *J. Phys. Oceanogr.* **20**, 242–263 (1990).
- Bryden, H. L. & Pillsbury, R. D. *Computational Mech. Publs* (in the press).

ACKNOWLEDGEMENTS. This is a contribution to CNRS/INSU/JGOFS programme.

Derivation of some modern arc magmas by melting of young subducted lithosphere

Marc J. Defant* & Mark S. Drummond†

* Department of Geology, University of South Florida, Tampa, Florida 33620, USA

† Department of Geology, University of Alabama, Birmingham, Alabama 35294, USA

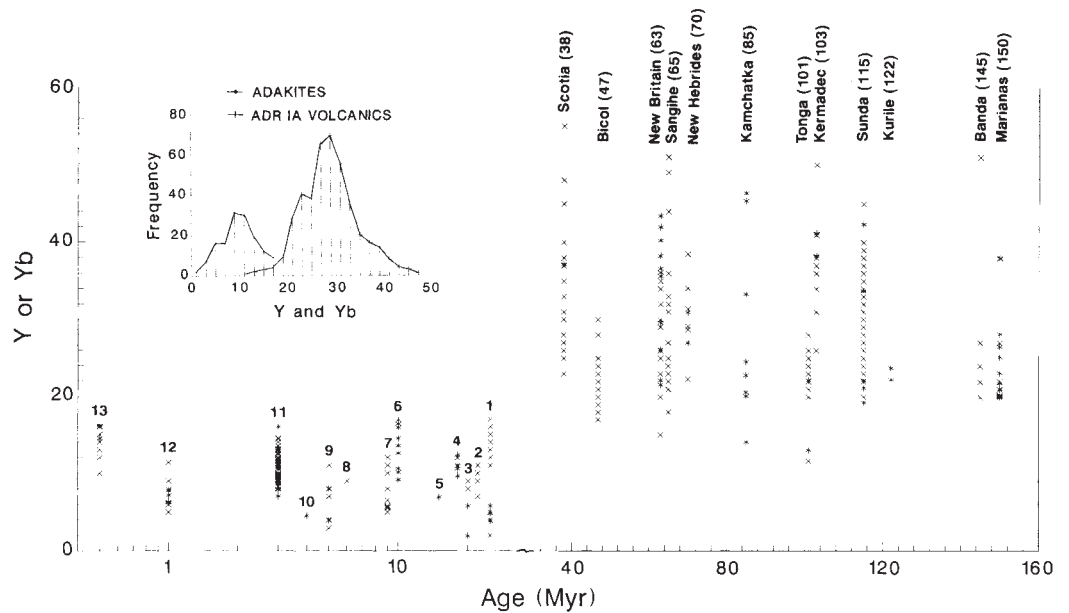
MOST volcanic rocks in modern island and continental arcs are probably derived from melting of the mantle wedge, induced by hydrous fluids released during dehydration reactions in the subducted lithosphere¹. Arc tholeiitic and calc-alkaline basaltic magmas are produced by partial melting of the mantle, and then evolve by crystal fractionation (with or without assimilation and magma mixing) to more silicic magmas²—basalt, andesite, dacite and rhyolite suites. Although most arc magmas are generated by these petrogenetic processes, rocks with the geochemical characteristics of melts derived directly from the subducted lithosphere are present in some modern arcs where relatively young and hot lithosphere is being subducted. These andesites, dacites and sodic rhyolites (dacites seem to be the most common products) or their intrusive equivalents (tonalites and trondhjemites) are usually not associated with parental basaltic magmas³. Here we show that the trace-element geochemistry of these magmas (termed 'adakites') is consistent with a derivation by partial melting of the subducted slab, and in particular that subducting lithosphere younger than 25 Myr seems to be required for slab melting to occur.

Gill¹ and Drummond and Defant³ have discussed the expected geochemical characteristics of rocks derived from the melting of subducted basalt. Experimental work indicates (see ref. 3 for a review) that the partial melting of metamorphosed basalt (amphibolite and eclogite) will produce relatively high-Al, mostly corundum-normative silicic melts ($\text{Al}_2\text{O}_3 > 15\%$ at 70% SiO_2). The existence of garnet or amphibole as a residual will lead to melts with low concentrations of yttrium and heavy rare-earth elements (HREEs).

The age of the lithosphere^{4,5} subducted along trenches associated with 12 island arcs is plotted against the concentrations of Y and normalized Yb in volcanics sampled from these arcs in Fig. 1. In all but nine samples (>400 samples plotted), the Y and normalized Yb values of the island-arc andesites, dacites and sodic rhyolites (ADRs) are ≥ 20 . Island arcs near continental margins, where subducted crustal sediments have been documented (such as Lesser Antilles arc⁶, Luzon arc, Philippines⁷, and Aleutian arc⁸) have been omitted because of the potential of lower Y and Yb values by source contamination. In these cases, however, only a few samples have Y and normalized Yb values < 20 .

Thirteen Cenozoic arc ADRs associated with young subducted crust (the crust subducted at the trench is ≤ 25 Myr old) have also been plotted in Fig. 1. All have Y and normalized Yb values < 19 , and most are < 15 . There are other volcanics that may fall into this group (such as the New Guinea Highlands and Eastern Papua, Papua New Guinea⁹, Kadavu Island, Fiji (ref. 10 and J. B. Gill, personal communication), and the Abu Volcano Group, Japan¹¹) but either the age of the subducted lithosphere is unknown or data are unavailable for these regions. Two general observations can be made. First, it is rare to find low Y and Yb concentrations in island-arc ADRs associated with subducted lithosphere older than 25 Myr. Second, in arcs where young crust is being subducted, ADR samples with both high and low Y and Yb can be found. For example, Mount St Helens has mostly low Y and Yb values but associated volcanoes in the Cascade range (not shown on the diagram because the Cascade arc is not an island arc) have higher values, comparable

FIG. 1 Y(*) and Yb(x) content of arc volcanics and plutonics plotted against the estimated age of the subducting lithosphere. Yb has been chondrite normalized²⁷ and multiplied by 2.4 to make the values approximately equivalent to Y values. Ages for the subducting crust^{4,5} associated with the Quaternary island arcs are given after the names in parentheses. The adakites are represented by numbers: 1, El Valle and La Yeguada volcanoes, Panama (25 Myr)^{13,28}; 2, Cook Island, Chile (22 Myr)²⁹; 3, Paracale pluton, Philippines (20 Myr) (M. J. D., unpublished data; samples from U. Knittel and W. Winter); 4, Austral Andes (18 Myr)^{30,31}; 5, Aleutian arc, dredged sample, Alaska (15 Myr)¹²; 6, Skagway batholith, Alaska (10 Myr)³²; 7, North Kamchatka (9 Myr)³³; 8, Sierra Madre, Mexico (6 Myr)³⁴; 9, Patagonia, Chile (5 Myr) (ref. 35 and D. S. Bartholomew, personal communi-



to those of the island arcs shown in Fig. 1.

We use the term adakite to describe these Cenozoic arc magmas because they were first documented in Adak Island (Aleutian Islands, Alaska)¹². They are volcanic or intrusive rocks in Cenozoic arcs associated with subduction of young (≤ 25 Myr) oceanic lithosphere. Adakites are characterized by $\geq 56\%$ SiO₂, $\geq 15\%$ Al₂O₃ (rarely lower), usually $< 3\%$ MgO (rarely above 6% MgO), low Y and HREE relative to island-arc ADRs (for example, Y and Yb ≤ 18 and 1.9 p.p.m., respectively), high Sr relative to island-arc ADR (rarely < 400 p.p.m.), low high-field strength elements (HFSEs), as in most island-arc ADRs, and $^{87}\text{Sr}/^{86}\text{Sr}$ usually < 0.7040 . The petrography of adakites is somewhat variable. Plagioclase is a ubiquitous phase, and amphibole is common in all samples but the more MgO-rich varieties. Clinopyroxene and orthopyroxene are also common constituents, with biotite and opaques occurring frequently. A common assemblage is plagioclase and amphibole (with or without biotite, pyroxene and opaques). Adakites are rarely associated with parent basalts or basaltic andesites. When they are, the basaltic rocks are usually extremely enriched in large-ion lithophile elements (such as absarokites and shoshonites¹³).

Trace-element modelling of the partial melting of basalt transformed to eclogite (with or without amphibolite) can explain the low Yb and Y values of adakites in Fig. 1. Various curves derived from fresh and altered MORB have been superimposed on a plot of Sr/Y against Y in Fig. 2. Most recent (Quaternary) island-arc ADRs do not resemble adakites even though both groups have comparable silica levels (Fig. 2). These arc volcanics seem to be derived from basaltic magmas originating from a metasomatized mantle-wedge source, perhaps enriched with a small sediment component. Basaltic melts, which have Sr and Y values comparable to adakites, probably differentiate by assimilation and fractional crystallization (AFC) (and magma mixing) towards more silicious compositions^{2,14}. The partial melting of a periodotitic source and subsequent differentiation is toward high Y concentrations (and low Sr/Y ratios) for island-arc ADR volcanics and opposite to that for formation of adakite by partial melting of metamorphosed basalt (see the AFC trend in Fig. 2).

Figure 3, a 'spider' diagram of an adakite, a representative normal-type MORB and two partial-melting curves from a

cation); 10, Los Chocoyos, Guatemala (4 Myr)³⁶; 11, Mount St Helens (3 Myr)³⁷; 12, Baja of California, Mexico (1 Myr)³⁸; 13, Woodlark Basin (0.5 Myr)³⁹.

MORB and a MORB and sediment (assuming a hornblende-eclogite restite)¹³, shows that trace elements can be modelled by partial melting of oceanic crust. There are strong positive Sr and Eu anomalies and depletions in Y and Yb in both the adakite and modelled melts.

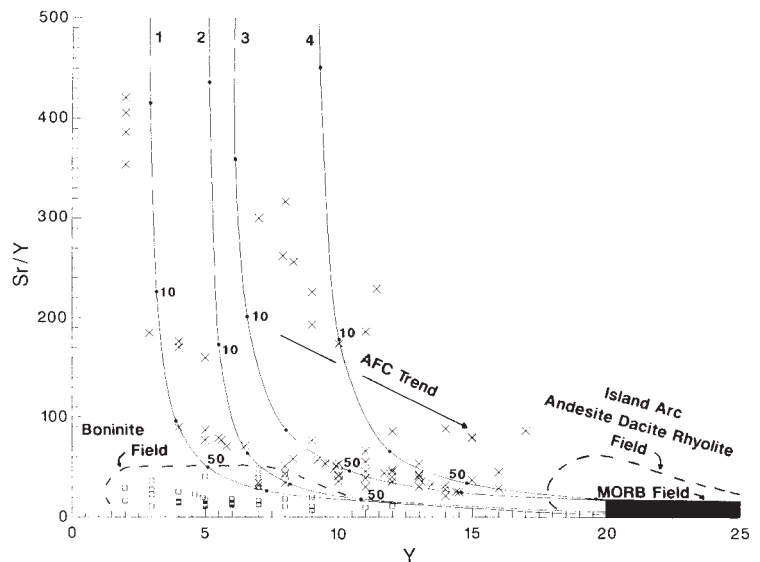
Although partial melting of subducted oceanic lithosphere seems to be the most internally consistent model for adakite generation, other types of petrogenesis are possible. The lower crust is a likely candidate because the geochemical signatures of adakites suggest a basaltic source. We contend, however, that partial melting of the lower crust by underplating will yield magmas with negative Eu anomalies and Al₂O₃ $< 15\%$ because basalt will not reach the amphibolite-eclogite transition under most arcs¹⁵. Similar geochemical signatures would be imparted to melts from plagioclase-rich granulite. Adakites have high Al₂O₃ ($> 15\%$) and absent or positive Eu anomalies (Fig. 3).

Partial-melting experiments on high-alumina basalts (possible lower-crustal rocks) indicate that adakites are not products of underplating¹⁶. Low-alumina (12.3% Al₂O₃) dacitic melts were generated by 5–10% partial melting (16 kbar and 1,050 °C under amphibole dehydration conditions). In contrast, partial melting of MORBs under subduction pressure and temperature conditions (20 kbar and 1,100 °C) produced high-alumina (17.2% Al₂O₃) dacitic material with higher degrees of partial melting (10–20%)¹⁶.

Some Mg-rich andesites are found in 5 of the 13 adakite localities (some as high as 6% MgO), but they are somewhat rare. Perhaps partial melting of the mantle wedge is the source of some adakites. Although adakites from a few locations have elevated Mg concentrations, they are not comparable to concentrations found in boninites (most boninites have $> 10\%$ MgO). Also, boninites have distinctive Sr/Y and Y values (Fig. 2) and are absent of plagioclase (adakites contain plagioclase). Differentiation of a boninite parent magma generates low-Al-type dacitic magmas (for example, the low-K rhyolites of Saipan¹⁷ or the quartz dacites from the Bonin Islands¹⁸), which are distinct from adakites (high-Al type).

Kay¹² has proposed a model that may explain the generation of the high-Mg subset of adakites: dacitic magmas generated by the melting of a subducted slab rise into the hot overlying mantle wedge where they re-equilibrate with peridotite under

FIG. 2 Sr/Y plotted against Y (adakites, \times ; boninites, \square). The curves represent various models of the partial melting of depleted and altered MORB with an amphibolite or eclogite residue: 1, eclogite (gt/cpx=50/50); 2, garnet amphibolite (gt/am=10/90); 3, amphibole eclogite (am/gt/cpx=10/40/50); 4, garnet amphibolite (gt/am=10/90). Starting compositions for curves 1 and 2: Sr=141 p.p.m. and Y=21 p.p.m.; curves 3 and 4: Sr=264 p.p.m. and Y=38 p.p.m. (see ref. 3 for further details). gt, garnet; cpx, clinopyroxene; am, amphibolite.



the hydrous conditions generating andesitic compositions. This process would explain the high-Mg content, relative to other adakites, and Y and HREE depletions found among this subset of rocks. Although we believe that the high-Mg adakites can be derived by the partial melting of the subducted slab without reaction with the mantle, we do not rule out Kay's alternative proposal. There is a continuum from low- to high-MgO adakites indicating that the high-Mg varieties are not unique. At any rate, these high-Mg adakites are a relatively small proportion of the adakites (<10% have MgO values ≥ 5 wt%). Further, partial melting of the mantle cannot be applied to the majority of adakites because of their relatively low MgO values (>75% have MgO values <4 wt%).

Modelling of fractional crystallization¹³ cannot explain the somewhat unique geochemistries of adakites. For example, plagioclase fractionation drives melts toward low Sr and high Y (Fig. 2) based on mineral-melt partition coefficients. Only amphibole and clinopyroxene can push magmas toward high Sr/Y and low Y, but these values cannot be reached if plagioclase fractionation along with the clinopyroxene and amphibole. Extensive amphibole fractionation (60%) is necessary to produce adakite REE compositions but 60% fractionation is inconsistent with the amount of amphibole normally found in adakites. Removal of this much subaluminous hornblende

would create a high-peraluminous felsic magma, which is inconsistent with the slightly peraluminous to metaluminous compositions of the adakites. Clinopyroxene is absent in many adakites and, therefore, it is difficult to see how fractionation of this mineral could generate adakites. Similar results are obtained when AFC or magma mixing processes are modelled¹³.

We conclude that the most likely derivation of adakites is from the partial melting of the subducted slab. This is supported by the existence of adakites associated with amphibolite and eclogite in exposed subduction zones. A melange complex, consisting of blocks of greenschist, blueschist, metagabbro, rhyolite (adakite), amphibolite and eclogite, has been described from Baja California Sur, Mexico¹⁹ beneath an Upper Triassic ophiolite. The Catalina schist of southern California is a subduction-zone metamorphic terrane. The interaction of fluids at high-pressure and temperature conditions initiated partial melting of metamorphosed basalt to generate trondhjemitic melts of adakite compositions in migmatitic blocks from the Catalina schist^{20,21}.

We suggest that only oceanic crust younger than 25 Myr is hot enough to initiate melting of the slab. Parsons and Sclater²² have plotted heat flow units (HFU) against the age of the oceanic crust. Crust younger than 25 Myr has HFU in the range ~2.8–8, but crust older than this has fairly constant HFU of 1–2.5.

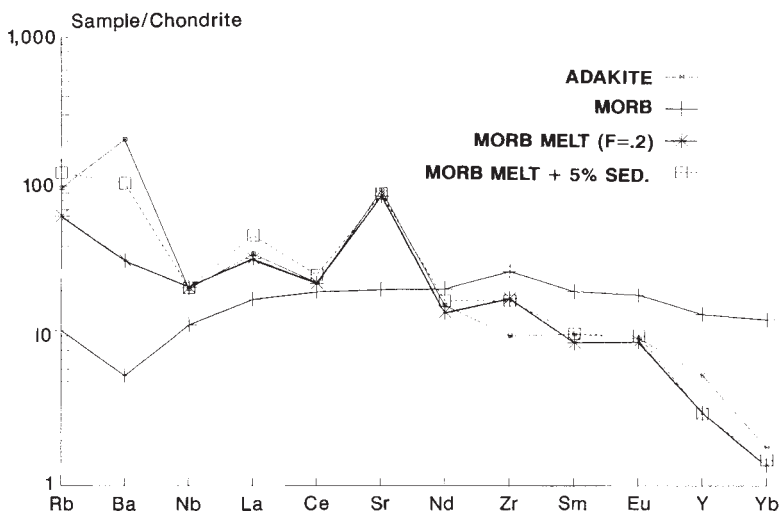


FIG. 3 Chondrite-normalized⁴⁰ compositions of a typical adakite and normal-type MORB and two models derived from 20% partial melting of the MORB and a mixture of 95% MORB and 2.5% marine sediments and/or 2.5% crustal sediments represented by an Archaean crustal component (see ref. 13 for details).

Perhaps subducted oceanic crust with HFU of at least 2.8 is needed to produce adakites during subduction. Based on phase diagrams and numerical heat-transfer models, Peacock²³ predicted that partial melting of the oceanic crust should occur "only within several tens of millions of years of the initiation of subduction in young oceanic lithosphere".

Archaean high-Al trondhjemites, tonalites and dacites have similar compositions to the adakites described above. The higher geothermal gradients in the Archaean probably led to the rapid generation and subduction of young hot crust. Partial melting of this subducted lithosphere may have been a dominant process in the production of dacitic and trondhjemitic compositions throughout the Archaean shield terranes^{3,24,25}.

Ellam and Hawkesworth²⁶ have suggested that "Either the continental crust is considerably more mafic than andesite, or the mechanism of crust formation has changed with time, such that a large proportion of the continental crust was formed by processes unlike those active in recent subduction zones." Adakites may be a modern analogue of Archaean magmatism. Their rarity in Cenozoic arcs can be related to the scarcity of subduction of young oceanic crust, explaining why the generation of 'typical' continental crust material is rare in arc regions today. □

Received 4 April; accepted 23 August 1990.

- Gill, J. B. in *Orogenic Andesites and Plate Tectonics* (Springer, Berlin, 1981).
- Defant, M. J. & Nielsen, R. L. *Geochim. cosmochim. Acta* **54**, 87–102 (1990).
- Drummond, M. S. & Defant, M. J. *J. geophys. Res.* (in the press).
- Cande, S. C. et al. *Magnetic Lineations of the World's Ocean Basins* (map) (Am. Ass. Petrol. Geol., 1989).

- Scotese, C. R., Gahagan, L. M. & Larson, R. L. *Tectonophysics* **155**, 27–48 (1989).
- Davidson, J. P. *Geochim. cosmochim. Acta* **51**, 2185–2198 (1987).
- Defant, M. J., de Boer, J. Z. & Oles, D. *Tectonophysics* **145**, 305–317 (1988).
- Kay, R. W. *J. Geol.* **88**, 497–522 (1980).
- Smith, I. E. M., Taylor, S. R. & Johnson, R. W. *Contr. Miner. Petrol.* **69**, 227–233 (1979).
- Gill, J. B. *Earth planet. Sci. Lett.* **68**, 443–458 (1984).
- Tatsumi, Y. & Koyaguchi, T. *Contr. Miner. Petrol.* **102**, 34–40 (1989).
- Kay, R. W. *J. Volcan. geotherm. Res.* **4**, 117–132 (1978).
- Defant, M. J. et al. *J. Petrol.* (submitted).
- DePaolo, D. J. *Earth planet. Sci. Lett.* **53**, 189–202 (1981).
- Tepper, J. H. *Eos* **70**, 1420 (1989).
- Rapp, R. P., Watson, E. B. & Miller, C. F. (abstr.) *Goldschmidt Conf. Prog.* 69 (Geochem. Soc., Baltimore, 1988).
- Meijer, A. *Contr. Miner. Petrol.* **83**, 45–51 (1983).
- Kuroda, N., Shiraki, K. & Urano, H. *Contr. Miner. Petrol.* **100**, 129–138 (1988).
- Moore, T. E. *Geol. Soc. Am. Mem.* **164**, 43–58 (1986).
- Sorenson, S. S. *Metamorph. Geol.* **6**, 405–435 (1988).
- Sorenson, S. S. & Grossman, J. N. *Geochim. cosmochim. Acta* **53**, 3155–3177 (1989).
- Parson, B. A. & Sclater, J. G. *J. geophys. Res.* **82**, 803–827 (1977).
- Peacock, S. M. *Science* **248**, 329–337 (1990).
- Jahn, B. M., Vidal, Ph. & Kröner, A. *Contr. Miner. Petrol.* **86**, 398–408 (1984).
- Martin, H. *Geology* **14**, 753–756 (1986).
- Ellam, R. M. & Hawkesworth, C. J. *Geology* **16**, 314–317 (1988).
- Masuda, A., Nakamura, N. & Tanaka, T. *Geochim. cosmochim. Acta* **37**, 239–244 (1973).
- Defant, M. J. et al. *Contr. Miner. Petrol.* (in the press).
- Puig, A., Herve, M., Suarez, M. & Saunders, A. D. *J. Volcan. geotherm. Res.* **20**, 149–163 (1984).
- Stern, C. R., Skewes, M. A. & Duran, M. *Actas Primer Congreso Geologico Chileno* **2**, 195–212 (1976).
- Stern, C. R., Futa, K. & Muehlenbachs, K. in *Andean Magmatism—Chemical and Isotopic Constraints* (eds Harmon, R. S. & Barreiro, B. A.) 31–46 (Shiva, Cheshire, 1984).
- Barker, F., Arth, J. G. & Stern, T. W. *Am. Miner.* **71**, 632–643 (1986).
- Kepezhinskas, P. K. *Geologiya i razvedka* **1**, 59–65 (1988).
- Cameron, K. L. & Cameron, M. *Contr. Miner. Petrol.* **91**, 1–11 (1985).
- Bartholomew, D. S. thesis, Univ. Leicester (1984).
- Rose, W. I., Grant, N. K. & Easter, J. in *Ash-Flow Tuffs*, *Geol. Soc. Am., Spec. Pap.* 180, 87–99 (1979).
- Smith, D. R. & Leeman, W. P. *J. geophys. Res.* **92**, 10313–10334 (1987).
- Rogers, G., Saunders, A. D., Terrell, D. J., Verma, S. P. & Mariner, G. F. *Nature* **315**, 389–392 (1985).
- Johnson, R. W. et al. *Circum-Pacific Council for Energy and Mineral Resources, Earth Sci. Ser. Vol. 7* (eds Taylor, B. & Exon, N. F.) 155–226 (1987).
- Wakita, H., Rey, P. & Schmitt, R. A. *Proc. lunar Sci. Conf.* **2**, 1319–1329 (1971).

ACKNOWLEDGEMENTS. We thank U. Knittel for a review.

Transport of reef corals into the Great Barrier Reef

Paul L. Jokiel

University of Hawaii at Manoa, Hawaii Institute of Marine Biology,
PO Box 1346, Kaneohe, Hawaii 96744, USA

MAJOR submarine pumice eruptions have occurred repeatedly during the past 25 years in the Tonga–Kermadec region^{1–3}. Pumice from this area drifts through Fiji and New Caledonia, reaching Australia roughly one year after an eruption^{1,2}. Coral larvae settle and grow on the floating pumice fragments (Fig. 1). The geographic pattern of abundance and size distribution of rafted corals found on drift pumice in relation to the pumice source area suggests massive transport of corals into the Great Barrier Reef from regions of lower diversity lying far to the east and southeast. Dispersal range is not limited by longevity of larvae and centres of diversity may be sites of species accumulation rather than sites of species origin.

Mean colony diameter, maximum diameter, size range, standard deviation of the mean, and abundance of coral settlements found on drift pumice increase with increasing distance along the drift trajectory (Table 1 and Fig. 2). Differences in the distributions for each pair of locations are significant ($P < 0.001$ by the Kolmogorov–Smirnov two-sample test for distributions⁴), suggesting continuous growth of colonies after settlement with additional recruitment throughout the drift period. The largest rafted corals found in Australia have a diameter of ~2 cm. Corals of this size are about one year old^{5,6}, which is consistent with directly observed drift time for the pumice.

Corals of the family Pocilloporidae accounted for 70% of the total, with the genera *Pocillopora*, *Seriatopora* and *Stylophora* being represented. Acroporidae accounted for 25% of the total. The genus *Acropora* was abundant and several colonies of *Montipora* were clearly identifiable. The remaining 5% consisted

TABLE 1 Size and numbers of rafted corals collected per unit effort at various locations

Location	n	Mean ± s.d. (mm)	Range (mm)	Rafted corals collected	
				per h	per km
New Zealand	0	0	0	0	0
Fiji	15	1.5 ± 0.4	0.9–2.2	1	2
New Caledonia	12	2.9 ± 1.4	1.3–6.2	3	4
Australia	156	5.2 ± 4.8	0.5–22.0	5	10

of colonies of Poritidae (*Porites* and *Goniopora*) and Faviidae (*Favia* and *Cyphastrea*).

Pumice fragments that carried corals into the Great Barrier Reef have the distinctive elemental composition of pumice known to originate in the Tonga region (Table 2), and is unlike pumice that originates in other geographic regions^{1,7}. The major surface currents between Tonga and the Great Barrier Reef flow to the southwest (Trade Wind Drift), developing into a strong southerly current (East Australia Current) near the coastline of Australia, which eventually joins the Tasman Current flowing eastward to New Zealand^{8,9}. The observed drift trajectory of pumice actually approximates the pattern of surface wind in the region¹⁰, rather than the published generalized pattern of surface currents. Pumice drift direction is controlled by current direction rather than wind direction¹. The apparent contradiction is readily explained. Wind stress in the southeast Trade Wind region drags the shallowest layer of water, which contains the pumice, to the northwest. The deeper layers are increasingly deflected to the southwest with increasing depth due to the Coriolis effect and shear phenomena as described by the 'Ekman spiral'¹¹. Reported 'surface current' shown in generalized maps of net surface water transport actually represents integrated transport above the thermocline. The result is massive transport of corals into the Great Barrier Reef, suggesting that centres of high diversity may actually represent centres of species accumulation rather than centres of species origin^{12–14}.